Role of Charge Regulation and Size Polydispersity in Nanoparticle Encapsulation by Viral Coat Proteins

ARTICLE *in* THE JOURNAL OF PHYSICAL CHEMISTRY B · JANUARY 2015

Impact Factor: 3.3 · DOI: 10.1021/jp5108125 · Source: PubMed

THE JOURNAL OF PHYSICAL CHEMISTRY B

Article

pubs.acs.org/JPCB

Role of Charge Regulation and Size Polydispersity in Nanoparticle Encapsulation by Viral Coat Proteins

Remy Kusters,[†] Hsiang-Ku Lin,[‡] Roya Zandi,[‡] Irina Tsvetkova,[§] Bogdan Dragnea,[§] and Paul van der Schoot*[,†,∥]

[†]Faculteit Technische Natuurkunde, Technische Universiteit Eindhoven, Postbus 513, 5600 MB Eindhoven, The Netherlands

[‡]Department of Physics and Astronomy, University of California—Riverside, Riverside, California 92521, United States

[§]Department of Chemistry, Indiana University, 800 E. Kirkwood Avenue, Bloomington, Indiana 47405, United States

[∥]Instituut voor Theoretische Fysica, Universiteit Utrecht, Leuvenlaan 4, 3584 CE Utrecht, The Netherlands

ABSTRACT: Nanoparticles can be encapsulated by virus coat proteins if their surfaces are functionalized to acquire a sufficiently large negative charge. A minimal surface charge is required to overcome (i) repulsive interactions between the positively charged RNA-binding domains on the proteins and (ii) the loss of mixing and translational entropy of RNA and capsid coat proteins. Here, we present a model describing the encapsulation of spherical particles bearing weakly acidic surface groups and investigate how charge regulation and size polydispersity impact upon the encapsulation efficiency of gold nanoparticles by model coat proteins. We show that the surface charge density of these particles cannot be assumed fixed, but that it adjusts itself to minimize electrostatic repulsion between the charges on them and maximize the attractive interaction with the RNA binding domains on the proteins. Charge regulation in combination with the natural variation of particle radii has a large effect on the encapsulation efficiency: it makes it much more gradual despite its inherently cooperative nature. Our calculations rationalize recent experimental observations on the coassembly of gold nanoparticles by brome mosaic virus coat proteins.

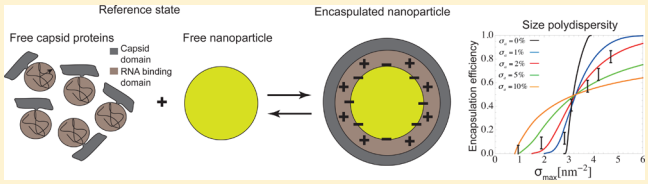

INTRODUCTION

In its simplest form, a virus consists of a single-stranded RNA enclosed in a more or less spherical proteinaceous container known as the capsid. Typically, the capsid is built up from many copies of a single viral coat protein. The coat proteins of many simple viruses have a disordered, positively charged RNA-binding domain also known as arginine-rich motif (ARM) that makes direct contact with the negatively charged RNA.[1] There are strong indications that the assembly of viruses is predominantly driven by generic electrostatic interactions.[2−5] In addition, specific interactions involving packaging signals on the RNA may play a role in either speeding up the assembly or even stabilizing the capsid by inducing conformational changes in the coat proteins.[6−8]

In view of this, it is not surprising that coat proteins of a number of (plant) viruses have shown the ability to encapsulate in vitro not only their native RNAs but also heterologous ones,[9] negatively charged polymers,[10,11] DNA,[12] supramolecular polymers,[13,14] emulsion droplets stabilized by anionic surfactants, and surface-functionalized nanoparticles.[15,16] Clearly, from the perspective of obtaining a fundamental understanding of the physical principles that dictate the efficiency of the spontaneous encapsulation, by far the simplest system would be that where the cargo comprises solid nanoparticles. The reason is, of course, that these do not change their molecular structure and/or size, in contrast to, e.g., single-stranded RNA or other types of polyanion.[1,14] The spontaneous encapsulation of negatively charged particles is also of technological interest with potential applications in medical imaging, metamaterials, and controlled drug release.[13,17,18]

Recent experiments[17] have shown that both the size and surface charge density of the nanoparticles have a crucial impact on the encapsulation by brome mosaic virus (BMV) coat proteins. Indeed, irrespective of nanoparticle size, a minimal surface charge density seems to be required for encapsulation, at least under conditions of low pH, although decreasing the size of the nanoparticle from 12 to 6 nm does decrease the encapsulation efficiency significantly.[15−17,19] The acidity of the solution is crucial here, as titration experiments indicate that for near-neutral pHs the assembly seems to follow a Langmuir isotherm, whereas for acidic pH values it obeys a Hill-type process.[17] The obtained Hill coefficient of 90 suggests a cooperative all-or-nothing adsorption assembly of the dimeric coat proteins onto particles of 11 nm diameter, corresponding to $T = 3$ virus-like particles consisting of 180 proteins. Interestingly, despite the high degree of cooperativity at low pH, the efficiency of encapsulation is a gradual function of the surface charge density of the nanoparticles, and more so the smaller the nanoparticles.[17]

Received: October 28, 2014
Revised: January 6, 2015
Published: January 6, 2015

DOI: 10.1021/jp5108125
J. Phys. Chem. B 2015, 119, 1869−1880

To control the surface charge density, the particles are functionalized by end-grafting onto them poly(ethylene glycol) molecules (PEGs) with two different kinds of end group. One involves a weakly acidic carboxyl (COOH) group and the other a hydroxyl (OH) group.[17,20] The former may dissociate at pH values in excess of its pK_a and in that case become negatively charged. The surface charge density can be controlled, at least in principle, by varying the pH at fixed ratio of the number of carboxyl and hydroxy end groups on the surface of the particles, or, alternatively by varying this ratio at fixed pH. Indeed, the degree of dissociation varies with the surface density of the carboxyl groups, the kind and concentration of mobile ions in the solution, the size of the nanoparticles, and so on. In fact, the degree of dissociation of carboxyl groups on naked nanoparticles differs from those on encapsulated ones because of the proximity of the positive charges on the ARMs of the capsid proteins.[3] This is a result of what is known as charge regulation.[20]

There have been a number of theoretical papers dealing with the encapsulation of charged nanoparticles by virus coat proteins.[3,5,21,22] Most of the experimental findings can be rationalized by the model calculations based on Poisson−Boltzmann (or Debye−Hückel) theory for the electrostatics,[5,21] in some cases applied within the context of the law of mass action describing the coassembly of proteins and nanoparticles.[3,23] While qualitatively in agreement with the available experimental data, the cited works cannot explain the gradual increase of the encapsulation efficiency with increasing surface charge density beyond the critical value. A solution to this problem was recently proposed by Lin et al.,[22] who put forward that charge regulation leads to a distribution of surface charge density on the nanoparticles around the average value. This is due to the intrinsically statistical character of charge regulation, where the degree of dissociation of ionizable groups on the surface of the nanoparticles responds on one hand to the solution conditions and on the other to the charged state of the nanoparticles themselves.[24] The width of the distribution of surface charge density scales with the inverse of the square root of the number of ionizable groups on the particles, which for nanoparticles is not a large number.[22] While the work of Lin et al.[22] does describe available experimental data rather well, it does not give a complete description of charge regulation and in principle is valid only for low charge densities.

In this paper, charge regulation on the nanoparticles is implemented rigorously through a simple statistical acid−base equilibrium model that responds to interactions with all other charges present, i.e., those on the nanoparticles and on the ARMs, and those present in the solution. For this purpose, we solve the relevant Poisson−Boltzmann equation analytically in the Debye−Hückel limit of low surface charge densities and find it in reasonable agreement with a numerical evaluation of the nonlinear Poisson−Boltzmann equation for a charge-regulated cargo. The advantage of the Debye−Hückel approximation is that we are able to obtain analytical expressions for the shift of the effective pK_a as a function of particle radius and density of acidic groups. Our calculations confirm that the mean surface charge density of the weakly acidic groups on the surface of the nanoparticles, which drive the assembly, cannot be assumed constant in the encapsulation process but adjusts itself to minimize electrostatic self-interactions and maximize the attractive interactions with the RNA-binding domain. Not surprisingly, this quite strongly influences the functional dependence of the encapsulation efficiency on the surface density of chargeable groups on the nanoparticles. In contrast with earlier theoretical work,[3,5,21,22] we do account for the full reference state in our free energy calculation; that is, we not only account for the electrostatics of the free nanoparticles but also that of the free coat proteins. We find that, in subtracting from the electrostatic free energy of the virus-like particles (VLP), that of the free proteins and nanoparticles is crucial for a realistic description for nanoparticle encapsulation efficiency.

Another important experimental fact that has not been addressed in any of the quoted theoretical descriptions is that of the natural variations in nanoparticle size. Indeed, Daniel et al. have reported that the size of the nanoparticles is approximately normally distributed with a standard deviation of almost 10%.[17] Here, we show that while such a standard deviation may seem quite narrow, it actually has a very strong impact on the encapsulation efficiency as a function of the surface density of chargeable groups, an impact that is at least as strong as that of a charge distribution on particles of equal size.[22] Our theory compares favorably with findings of recent assembly experiments.[17]

The remainder of this paper is organized as follows. In the Theory section, we present our model for nanoparticle encapsulation, and outline our calculations of the free energy of the encapsulated particles and its reference state. The results of the charge regulation and the influence of a distribution in particle size will be presented in the Results. In the Discussion and Conclusions section we summarize our work and present the main conclusions.

THEORY

In order to obtain a theoretical description of the efficiency of encapsulation of nanoparticles by viral coat proteins we invoke the law of mass action, which accounts for the loss of translational and mixing entropy of the free protein subunits and the nanoparticles, and calculate the relevant association constant by evaluating the gain in electrostatic free energy upon encapsulation. As already advertised in the preceding section, encapsulation is primarily driven by electrostatic interactions between positive charges located on the disordered RNA-binding domain of the protein subunits and negative charges associated with the weakly acidic groups on the surface of the nanoparticle.[2−5] To calculate the contribution to the free energy from the Coulomb interactions, we explicitly account for the attraction between the positive and negative charges, for the repulsive electrostatic interactions between the RNA-binding domains in the fully formed capsid, and for the repulsive interactions between the weakly acidic groups on the surface of the nanoparticle. From this we subtract the electrostatic free energy of the reference state that constitutes a free nanoparticle and the number of free protein subunits necessary to encapsulate a single nanoparticle. Our model is schematically represented in Figure 1.

The nanoparticles are considered to be perfect spheres with an effective radius a, which is the sum of the bare radius of a nanoparticle plus the height of the weakly acidic ligands grafted onto it. We denote σ_{max}, the surface density of ligands that bear an ionizable group. The capsid is modeled as a hollow spherical thick shell consisting of a homogeneously charged region $a < r < b_{in}$, representing the positive charges on the RNA-binding domains, and a shell consisting of the assembly domains of the coat proteins for $b_{in} < r < b_{out}$, the latter having a relative dielectric permittivity of $\varepsilon_p = 5$.[25] Here, b_{in} and b_{out} are the

DOI: 10.1021/jp5108125
J. Phys. Chem. B 2015, 119, 1869−1880

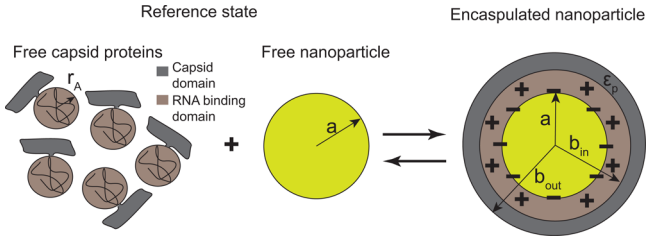

Figure 1. Illustration of the encapsulated nanoparticle and its reference state. The encapsulated nanoparticle is represented by a perfect sphere with radius a, surrounded by a homogeneously charged region $a < r < b_{in}$, where the RNA-binding domains of the coat proteins reside. The RNA-binding domain region is surrounded by a spherically symmetric shell of outer radius b_{out}, representing the region where the assembly domains of the coat proteins are situated. The shell has an estimated relative dielectric permittivity of $\varepsilon_p = 5$, through which salt can penetrate in the RNA-binding domain region. The reference state consists of a single spherical nanoparticle and q coat proteins required to encapsulate a single nanoparticle.

inner and outer radii of the protein shell, and r denotes the radial position.

Mobile salt ions are allowed to penetrate through holes in the capsid and enter the shell where the RNA-binding domains reside. We do not explicitly model the presence of the holes. We neglect the negative charges present on the outer surface of the shell as they contribute relatively little to the overall electrostatics of the problem.[25] To calculate the radius of the ARM region, r_A, in free solution, we model them as flexible polyelectrolytes and determine r_A by considering the competition between the configurational entropy of a short Gaussian chain and the Coulomb self-energy. In our electrostatic description of the free proteins, we only take into account the contribution of the ARM region and ignore all the other charges on the capsids. The details of the calculations are given in Appendix A.

We now proceed describing the law of mass action for our specific system of nanoparticle encapsulation. For simplicity we presume that the nanoparticle is either "naked" or completely covered by the protein shell. This is reasonable as the encapsulation is highly cooperative, at least for the pH of 4.5 where the experiments are done.[16,17] Indeed, experimental findings point at the existence of a critical surface charge density below which no encapsulated nanoparticles are observed, justifying our "all-or-nothing" model.[17] This, and the absence of spontaneously formed capsids, indicates that the attractive interactions between the proteins must be strong, yet not strong enough to induce spontaneous assembly at the molar fraction of dimeric coat protein of about 1.8×10^{-7} at which the assembly experiments were performed.[17] Attractive interactions between the proteins are likely to be dominated by hydrogen-bonded carboxyl/carboxylate pairs and/or carboxylates bound by Ca^{2+} or Mg^{2+} ions.[12]

Our "all-or-nothing" assembly model is similar to that presented previously by van der Schoot et al.,[2] Hagan,[3] and Zandi et al.,[23] and connects the encapsulation efficiency η to (i) the net protein−protein binding free energy difference, ΔG, (ii) the net difference in electrostatic free energy, ΔF, upon assembly in a single VLP, and (iii) the concentration of nanoparticles and coat proteins in the solution. ΔG and ΔF are free energy differences presumed to be negative, scaled to the thermal energy and hence dimensionless. Within our model assumptions, the encapsulation efficiency, η, then obeys the following Hill-type mass action equation[22]

$$\left(\frac{\eta}{1-\eta}\right)^{1/q} \frac{1}{(\varphi_{CP} - \eta q \varphi_{NP})} = \exp[-\Delta F - \Delta G] \equiv K \tag{1}$$

with q the number of protein subunits necessary to encapsulate a single nanoparticle, φ_{NP} the mole fraction of nanoparticles in solution, and φ_{CP} that of the protein subunits. (Note that for BMV the protein subunits are dimeric.) From eq 1, we deduce that the assembly efficiency rises sharply with protein concentration if $\varphi_{CP} > K^{-1}$, where K^{-1} can be seen as a critical association concentration. In fact, if $\varphi_{CP} < K^{-1}$, $\eta \sim 0$, if $\varphi_{CP} > K^{-1} + q\varphi_{NP}$, $\eta \sim 1$, and for $K^{-1} < \varphi_{CP} < K^{-1} + q\varphi_{NP}$, η is linear in φ_{CP} with $\eta \sim (\phi_{CP} - K^{-1})/q\phi_{NP}$.[23] Titration experiments confirm the validity of eq 1 at least for charged gold nanoparticles encapsulated by BMV.[16,26] Clearly, the important control parameter is $K = \exp[-\Delta F - \Delta G]$. ΔG cannot straightforwardly be calculated form any coarse-grained model, so we will leave it as a free parameter (see, however an attempt by Kegel et al.[27]). In principle it can be estimated from the critical concentration at which empty capsids form under conditions of high ionic strength.[12] For CCMV it is about $-17k_BT$.[16]

The dimensionless free energy ΔF, normalized to k_BT and describing the electrostatic driving force of assembly, is the sum of a dissociation free energy difference, ΔF_d, related to the chargeable groups on the surface of the nanoparticle and the electrostatic (Coulomb) free energy difference, ΔF_C

$$\Delta F = \Delta F_d + \Delta F_C \tag{2}$$

The free energy ΔF_d measures the difference between the dissociation free energy of the chargeable groups on the nanoparticles in a capsid and that in free solution. Let a fraction f of the end-groups be deprotonated and hence charged, and let a fraction $1-f$ be protonated. If the protons on the carboxyl groups are in chemical equilibrium with those in free solution, then within simple mean-field theory we can write for the dissociation free energy

$$F_d(f) = 4\pi a^2 \sigma_{max}[f \ln f + (1-f)\ln(1-f) + g(1-f) - \mu(1-f)] \tag{3}$$

in which a is again the radius of the nanoparticle, σ_{max} is the surface density of weakly acidic groups, $f \ln + f + (1-f)\ln (1-$ f) describes the contribution from the mixing entropy of the protonated and deprotonated acidic groups on the surface of the nanoparticle, and $g(1-f)$ is the binding free energy of the hydronium ions to carboxylate groups. The binding free energy can be related directly to the bare pK_a^0 of the weakly acidic ligands free in solution, because $g = -\ln 10 \times pK_a^0$. The third term, $\mu(1-f)$, denotes the chemical potential of the hydronium and can directly be related to the pH of the buffered solution through the relation $\mu = \ln 10 \times pH$.[28]

If we optimize eq 3, we obtain the well-known Henderson−Hasselbalch equation. However, the fraction of charged groups f depends not only on the pH and pK_a^0, but also on the charged state of the entire particle. Screened Coulomb interactions between carboxyl groups shift the effective pK_a away from the bare value, pK_a^0, a phenomenon also known as charge regulation.[20] To distinguish between chargeable groups on the bare nanoparticles and those encapsulated in the virus-like

DOI: 10.1021/jp5108125
J. Phys. Chem. B 2015, 119, 1869−1880

particles, we introduce f_{NP} and f_{VLP} for the fraction of charged groups in these two cases. The relative dissociation free energy (scaled to the number of proteins that make up the shell) must therefore be equal to

$$\Delta F_d \equiv [F_d(f_{VLP}) - F_d(f_{NP})]/q \quad (4)$$

where the values for f_{NP} and f_{VLP} are determined by minimization of the free energy ΔF, as we show in the next section, and where the division by the aggregation number q is because ΔF and ΔF_d hence are defined on a per protein basis. Before we can pursue this, we need to calculate the relative electrostatic (Coulomb) free energy ΔF_C.

To calculate the net difference in electrostatic free energy ΔF_C of the encapsulated nanoparticle with respect to that of its reference state, we invoke Poisson−Boltzmann theory and integrate the electrostatic potential $\psi(\vec{r})$ over the positions of the charges on the surface of the nanoparticle $\sigma_{max} f\, dS$ and those of the charges that reside in the RNA-binding domain region ρdV. The bare free energy is then given by

$$F_C = \int \rho\psi(\vec{r}, \rho)\, dV + \int \sigma_{max} f\psi(\vec{r}, \sigma_{max} f)\, dS \quad (5)$$

which we apply to the encapsulated particle, the naked particle, and the free protein units. Here, $\rho = Q/(4\pi(b_{in}^3 - a^3)/3)$ denotes the homogeneous charge density in the RNA-binding domain, σ_{max} the surface density of weak acidic groups, f the degree of dissociation of the ionizable groups, and ψ the electrostatic potential. The radius r_A and their corresponding free energy F_C of the RNA-binding domain free in solution is determined by a competition between the electrostatic repulsion and the configurational entropy of the chain. (In Appendix A we outline this calculation.) Focusing first on the electrostatics in the Debye−Hückel approximation, and referring to Appendix A for details on the calculations, we find

$$\begin{aligned} q\Delta F_C = &-\left(\frac{12\pi a^2 \lambda_D^2 \lambda_B}{b_{in}^3 - a^3}\right)[a - b_{in} e^{-(b_{in}-a)/\lambda_D}]\sigma_{max} f_{VLP} Q \\ &+ 8\pi^2 \lambda_D \lambda_B a^2 \sigma_{max}^2 (f_{VLP}^2 - f_{NP}^2) \\ &+ \left[\frac{3\lambda_D^2 \lambda_B}{2(b_{in}^3 - a^3)} - \left(\frac{3\lambda_D^2 \lambda_B}{2qr_A^3}\right)\right] Q^2 \end{aligned} \quad (6)$$

valid in the asymptotic limit of a, $b_{in} \gg \lambda_D$ and $b_{out} - b_{in} \ll \lambda_D$, i.e., near physiological conditions. The Bjerrum length equals about $\lambda_B \approx 0.7$ nm in water at room temperature, and the Debye length $\lambda_B \approx 0.3/(c_s)^{1/2}$ nm for the concentration of (monovalent) salt c_s [M].

The first term in eq 6 accounts for the attractive interaction between the negatively charged surface and the positively charged RNA-binding domains that drive the assembly, the second accounts for the self-energy of the negative charges present on the surface of the nanoparticles, while the third accounts for the self-energy of the positive charges on the RNA-binding domains. Note that eq 6 properly accounts for the contributions of the reference state, as explained above. Several conclusions can already be drawn from it: (i) if $\sigma_{max} \to 0$ the last term dominates, so $\Delta F_C > 0$ and assembly is unfavorable; (ii) for $\Delta F_C < 0$, σ_{max} needs to be large enough for the first term to compensate for the last term, but not too large as in that case the second term will predominate and result in $\Delta F_C > 0$, implying that assembly is unfavorable. In conclusion, eq 6 shows that a minimal σ_{max} is needed to get coassembly of coat proteins and nanoparticles into VLPs, which is in agreement with experiments.[17] Precise conditions depend on a whole host of parameter values, which depend on the particular system of interest. It is important to point out that ΔF_C depends very strongly on the magnitude of the gap between nanoparticle and the inner surface of the capsid, $b - a$. We return to this in the following section.

We are now in a position to optimize the total free energy ΔF with respect to the fraction of ionized groups on the encapsulated and free particle, f_{VLP} and f_{NP}, by setting $\partial\Delta F/\partial f_{NP} = \partial\Delta F/\partial f_{VLP} = 0$. Inserting the equilibrium values of f_{VLP} and f_{NP} back into 6, we obtain the actual free energy of encapsulation, that is, the electrostatic contribution to that. Figure 2 shows the different contributions of the optimized free energy, i.e., the total ΔF, indicated by the roman numerical (III), bare free energy without the contribution from the coat proteins in free solution (II), and a bare free energy ignoring the reference state completely (I), as has been done in previous literature.[3,5,22] For comparison we choose our parameters to model the experiments of Daniel et al., i.e., a nanoparticle with radius $a = 9.0$ nm encapsulated by a $T = 3$ BMV capsid, where we estimate $b_{in} = 11.3$ nm, $b_{out} = 13$ nm, pH − $pK_a^0 = 1.5$, $q = 90$, and $Q = 1620$.[17]

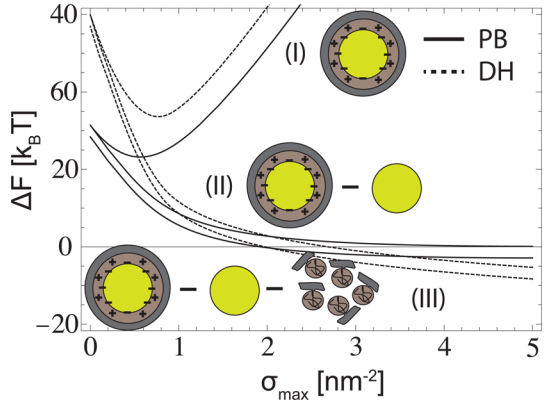

Figure 2. Electrostatic free energy difference ΔF per virus coat protein for the encapsulation by a $T = 3$ BMV capsid. The different curves show the electrostatic free energy of the encapsulated nanoparticle (I), the encapsulated nanoparticle relative to the free nanoparticle (II), and that relative to the whole reference state (nanoparticle and coat proteins) (III) in the Debye−Hückel approximation (dashed line) and the semianalytical analysis of the Poisson−Boltzmann equation discussed in the main text (solid line). In this example we presume that pH − $pK_a = 1.5$, the radius of the nanoparticle of $a = 9.0$ nm, the inner radius of the capsid of $b_{in} = 11.3$ nm, the outer radius of the capsid of $b_{out} = 13$ nm, the Bjerrum length $\lambda_B = 0.7$ nm, the Debye length $\lambda_D = 1.2$ nm, and the number of charges in the RNA-binding domain equal to $Q = 1620$, corresponding to $q = 90$.[17]

The figure illustrates the importance of properly including the reference state in the calculation of the effective electrostatic free energy, in particular accounting for the self-energy of the free protein subunits that so far has been ignored in the literature, as already alluded to. It can also be seen that the lowest value of σ_{max} for this system for which $\Delta F > 0$, a necessary condition for assembly, is around 2 nm^{-2}, which is close to the values reported by previous Poisson−Boltzmann and Debye−Hückel treatments[3,5,22] and experiments[17] for this specific system.

As is well-known, the Debye−Hückel theory that we invoke is valid for low values of the electrostatic potential only, and its

DOI: 10.1021/jp5108125
J. Phys. Chem. B 2015, 119, 1869−1880

accuracy in describing the encapsulation of charged nanoparticles has been questioned in the past, because the electrostatic potential in the ARM region is not necessarily small.[5,21,25] However, in our case we would still expect it to hold because of the charge regulation. The reason is that the ionizable groups on the surface of the nanoparticles have the ability to dissociate charges and therefore seek a charge distribution with the lowest possible total electrostatic free energy, which is precisely the regime where the linearized Poisson−Boltzmann theory is expected to hold.

Indeed, while not exact, our Debye−Hückel calculations do compare well with a semianalytical analysis of the Poisson−Boltzmann equation and a numerical evaluation of the free energy. We do not invoke a full numerical solution of the Poisson−Boltzmann equation, in view of the computationally costly free energy minimalization that should be repeated for every integration step in the calculation of the overall electrostatic free energy. Rather, we use a semianalytical approach for the electrostatic potential that turns out to compare very well with numerical studies.[25,29] It is based on descriptions by Prinsen et al.[25] for multishell capsids and by Tuinier[29] for charged spherical particles with fixed surface and volume charge distributions. The former hinges on the fact that the total number of fixed charges in the RNA-binding region is much larger than that of the mobile ions due to counterion release, allowing us to treat the influence of the latter perturbatively. The interior of the protein shell itself is assumed to contain no free charges, so in this region the problem reduces to a Poisson problem. Outside the capsid, the electrostatic potential is sufficiently small to allow for a Debye−Hückel approximation.[25]

To calculate the electrostatic potential of the free nanoparticle, we use an exact analytical solution of the Poisson−Boltzmann equation for a flat geometry and correct it with an ad hoc curvature term put forward by Tuinier that turns out to compare very well with a numerical evaluation of the Poisson−Boltzmann equation, at least if the radius of the nanoparticle is larger than the Debye length, which applies to our case.[29]

In Figure 2 we compare our treatment of the Poisson−Boltzmann equation (solid lines) with the Debye−Hückel approximation (dashed lines) for the enapsulation of a 9.0 nm radius nanoparticle in a typical $T = 3$ BMV capsid, assuming conditions similar to those of the experiments by Daniel et al.[17] For this set of parameters we see that the Debye−Hückel approximation describes the trend quite well even at high values of σ_{max}. The discrepancy between the linear and nonlinear theory, at least for our system, is at most 5 times the thermal energy for values of the surface charge density above 1 nm^{-2} and below the experimentally realistic value of 5 nm^{-2}. For values of the surface charge density less than 1 nm^{-2}, the discrepancy is considerably larger. The accuracy of the Debye−Hückel approximation strongly diminishes for small σ_{max} as there are few negative charges to counter the positive charges in the RNA-binding domain region.

The discrepancy in this part of parameter space is not of great importance as $\Delta F > 0$, implying that encapsulation would anyway not occur. The crossover from no assembly to potential assembly occurs if $\Delta F = 0$. For both DH and PB this happens for $\sigma_{max} \approx 2$ nm^{-2}. Assembly of empty capsids occurs for concentrations $\varphi_{CP} > \exp[\Delta G]$. In the presence of nanoparticles the critical concentration is reduced by a factor of $\exp[\Delta F]$, which for $\sigma_{max} \approx 5$ nm^{-2} is equal to $e^{-10} \approx 10^{-5}$.

To conclude this section, we point at an important experimental fact that we address in the next section, which is the natural variation in nanoparticle size in actual encapsulation experiments, as reported by Dragnea and collaborators.[17] They find that for their nanoparticles the size is approximately normally distributed with a standard deviation of about 10%.[17] We shall make a comparison with the experimental findings of the Dragnea group,[17] and show that charge regulation combined with size polydispersity of the nanoparticles helps rationalize the experimental findings for the encapsulation efficiency as a function of the surface density of chargeable groups.

RESULTS

Charge Regulation. In the previous section we mentioned that the negative charges on the surface of the nanopaticles, necessary to drive the encapsulation by viral coat proteins, are obtained by end-grafted weakly acidic carboxyl (COOH) groups onto their surface.[17,20] These COOH groups dissociate at pH values in excess of their pK_a and become negatively charged. The degree of dissociation varies with surface density of the carboxyl groups σ_{max}, the kind and concentration of mobile ions in the solution, the size of the nanoparticle,[20] and the presence of the positively charged RNA-binding domain for the encapsulated nanoparticle. In fact, because of the presence of the positively charged RNA-binding domain, we have argued that the degree of dissociation of the carboxyl groups on naked nanoparticles, f_{NP}, differs from that of encapsulated ones, f_{VLP}. To quantify this, we minimize the total electrostatic free energy ΔF with respect to f_{VLP} for the encapulated nanoparticle and to f_{NP} for the free nanoparticle.

The degree of dissociation is related to the charged state of the particle, the bare pK_a of the weakly acidic groups, and the pH of the solution via a modified Henderson−Hasselbalch equation

$$\frac{f}{1-f} = \frac{f_{HH}}{1-f_{HH}} K_C \tag{7}$$

where f_{HH} is related to the bare pK_a of the weakly acidic groups that we denote pK_a^0, and the pH of the solution: $f_{HH}/(1-f_{HH}) \equiv \exp[(pH - pK_a^0) \ln 10]$ and K_C the Coulombic contribution to the degree of dissociation of the surface carboxyl groups. As we have discussed in the previous section, this is described by the electrostatic contribution to the free energy and in the Debye−Hückel approximation given by the expression

$$\ln K_C = -4\pi\lambda_D\lambda_B\sigma_{max}f_{NP} \tag{8}$$

for the free nanoparticle and

$$\ln K_C = -4\pi\lambda_D\lambda_B\sigma_{max}f_{VLP} + \frac{3\lambda_D^2\lambda_B}{b_{in}^3 - a^3}Q \tag{9}$$

for the encapsulated nanoparticle, provided that $b_{in}, a \gg \lambda_D$. If $\sigma_{max} \to 0$, from eqs 8 and 9 for the fraction of charged groups on the NP, we find the usual Henderson−Hasselbalch equation, $f_{NP} \sim 1/(1 + 10^{-pH+pK_a}) = f_{HH}$. For $\sigma_{max} \gg 1$, this modifies to $f_{NP} \sim f_{HH}/(1 + f_{HH}4\pi\lambda_B\lambda_D\sigma_{max}) = f_{HH}$, indicating if $4\pi\lambda_B\lambda_D\sigma_{max}f_{HH} \ll 1$ charge regulation effects are small, but if $\sigma_{max} > 1/\lambda_B\lambda_D f_{HH}$, the reverse is true.

For the same nanoparticle encapsulated in a capsid shell we find that because of the presence of the positively charged RNA-binding domain, the fraction of charged surface groups

DOI: 10.1021/jp5108125
J. Phys. Chem. B 2015, 119, 1869−1880

f_{VLP} is strongly enhanced until the surface charge density reaches the point where the total number of charges on the nanoparticles equals the number of positive charges in the proximity of the surface of the nanoparticle, i.e., within one Debye length. Equation 9 reveals that this happens when $\sigma_{max} f_{VLP} = 3\lambda_D Q/4\pi(b_{in}^3 - a^3)$. See also Figure 3C,D.

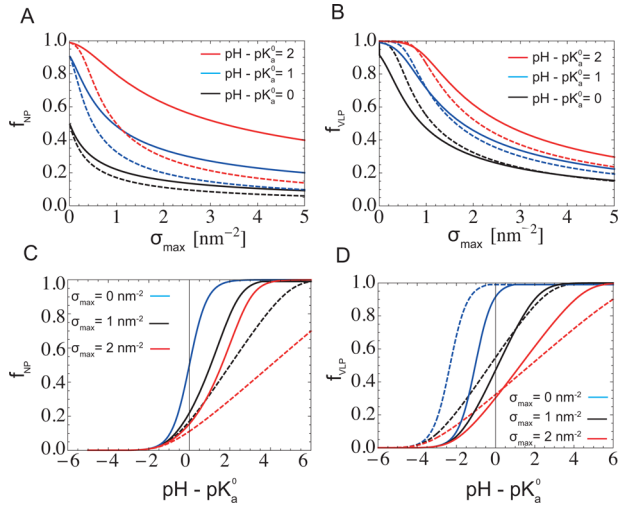

Figure 3. Fraction of charged groups on the surface of the nanoparticle as a function of the surface density of weakly acidic groups σ_{max} for (A) the free nanoparticle, f_{NP}, and (B) the nanoparticle encapsulated by a $T = 3$ BMV capsid, f_{VLP}. The dashed lines correspond to the Debye–Hückel approximation and the solid lines to our semianalytical analysis of the nonlinear Poisson–Boltzmann equation discussed in the main text. Increasing σ_{max} decreases the fraction of charged groups as a result of their Coulomb self-repulsion. In parts C and D we show the fraction of charged groups f_{NP} and f_{VLP} as a function of the pH − pK_a^0 for the free and the encapsulated nanoparticle, respectively. This shows that increasing the surface charge density shifts the apparent pK_a of the acidic groups. For the encapsulated nanoparticle there is an additional shift as a result of the proximity of the positively charged RNA-binding domain. Model parameters: $a = 8.7$ nm, $b_{in} = 11.6$ nm, $b_{out} = 13$ nm, $\lambda_B = 0.7$ nm, $q = 90$, $Q = 1620$, and $\lambda_D = 1.2$ nm, see also the main text.

For $\sigma_{max} \to 0$ we obtain a modified Henderson–Hasselbalch expression $f_{VLP} \sim K_c/(1 + 10^{-pH+pK_a})$, where $K_c = \exp(3\lambda_D^2\lambda_B Q/(b_{in}^3 - a^3)) > 1$ acts as a dissociation enlargement factor that renormalizes the bare pK_a of these groups. For $\sigma_{max} \gg 1$ we again obtain $f_{VLP} \sim f_{HH}/(1 + f_{HH} 4\pi\lambda_B\lambda_D\sigma_{max})$, similar to what we found for the free nanoparticle.

As can be deduced from eqs 8 and 9 and Figure 3, increasing the pH of the solution increases the fraction of charged groups for the free and encapsulated nanoparticles, but differently so. This is particulary true close to the pK_a, where a small shift in pH has a large impact on the degree of dissociation of the nanoparticle. Using eqs 8 and 9 and the fact that pH ≡ pK_a^0 at $f = 0.5$, it is possible to calculate within the Debye–Hückel theory the shift in effective pK_a of the weakly acidic groups on the surface of the nanoparticle relative to the bare value, pK_a^0

$$pK_a - pK_a^0 = +\frac{2\pi\lambda_D\lambda_B}{\ln 10}\sigma_{max} \qquad (10)$$

for the free nanoparticle, and

$$pK_a - pK_a^0 = +\frac{2\pi\lambda_D\lambda_B}{\ln 10}\sigma_{max} - \frac{3\lambda_D^2\lambda_B}{\ln 10(b_{in}^3 - a^3)}Q \qquad (11)$$

for the encapsulated nanoparticle. From eqs 10 and 11 and Figure 3 it follows that both for the free and the encapsulated nanoparticles, the upward shift in effective pK_a is linear in the surface density of weakly acidic groups. For the latter, there is also a downward shift proportional to the density of positive charges from the ARMs in the gap between the surface of the nanoparticle and the inner surface of the protein shell.

As we have mentioned before, predictions from the Debye–Hückel approximation (presented by the dashed lines in Figure 3) deviate from our semianalytical evaluation of the nonlinear problem (solid line in Figure 3). Figure 3A shows that for large values of pH − pK_a^0, the Debye–Hückel approach fails, in particular for large values of the surface charge density. The degree of dissociation for the encapsulated nanoparticles (Figure 3 C) from the Debye–Hückel theory compares well with the nonlinear theory, especially if the number of charges on the nanoparticles is compensated by an equal amount of positive charges in the RNA-binding domains located within one Debye screening length from the surface. For high values of σ_{max} we find that, similar to what we found for free nanoparticles in Figure 3A, the electrostatic interactions are overestimated.

Let us now explore how the encapsulation efficiency depends on the pH − pK_a. In Figure 4D we show that if we keep all system parameters constant, the critical σ_{max} above which assembly occurs increases upon increasing pH − pK_a. In this figure we put $a = 9.5$ nm, $b_{in} = 11.8$ nm, $q = 90$, $\varphi_{CP} = 1.8 \times 10^{-7}$, $\varphi_{NP} = 2.0 \times 10^{-9}$, $\lambda_D = 1.2$ nm, and for simplicity we set the binding free energy between the proteins $\Delta G = 0$. So, a small shift in the pK_a of the weakly acidic groups or the pH of the solution has a very strong influence on the encapsulation efficiency.

Finally, eq 11 reveals that the effective pK_a of weakly acidic groups on the encapsulated nanoparticle decreases as $1/(b_{in}^3 - a^3)$, indicating that this quantity and hence the surface charge density strongly depend on the size of the nanoparticle a relative to the inner radius of the capsid encapsulating it b_{in}. As we shall see next, this makes the encapsulation efficiencies exquisitely sensitive to the influence of particle size and polydispersity.

Size Polydispersity. To illustrate the effect of size polydispersity, we calculate within the Debye–Hückel theory the encapsulation efficiency, η, as a function of the surface density of weakly acidic groups σ_{max} from eq 1 for nanoparticles with slightly different radii: $a = 9.4$, 9.5, and 9.6 nm, encapsulated by a typical $T = 3$ BMV capsid, where we estimate $b_{in} = 11.8$ nm, $q = 90$, $Q = 1620$, $\varphi_{CP} = 1.8 \times 10^{-7}$, $\varphi_{NP} = 2.0 \times 10^{-9}$, $\lambda_D = 1.2$ nm, p$K_a^0 = 2.5$, and pH = 4.5.[17] We find that increasing the radius of the nanoparticle with only 0.1 nm increases its encapsulation efficiency strongly, without actually strongly affecting the shape of the curve. The critical σ_{max} above which assembly occurs decreases upon increasing the size of the nanoparticle. This is because, even at constant σ_{max}, the electrostatic interactions between the RNA-binding domain and the nanoparticles dominate over the increase in self-energy of the positive charges in the RNA-binding domain. This result is a direct consequence of the $1/(b_{in}^3 - a^3)$ dependence of the effective pK_a, see eq 11.

It is now clear that the encapsulation efficiency sensitively depends on the radius of the nanoparticle. This implies that the natural size polydispersity of the nanoparticles of up to 10% in the experiments by Daniel et al.[17] must have a significant impact on the assembly efficiency. To take into account the size

DOI: 10.1021/jp5108125
J. Phys. Chem. B 2015, 119, 1869–1880

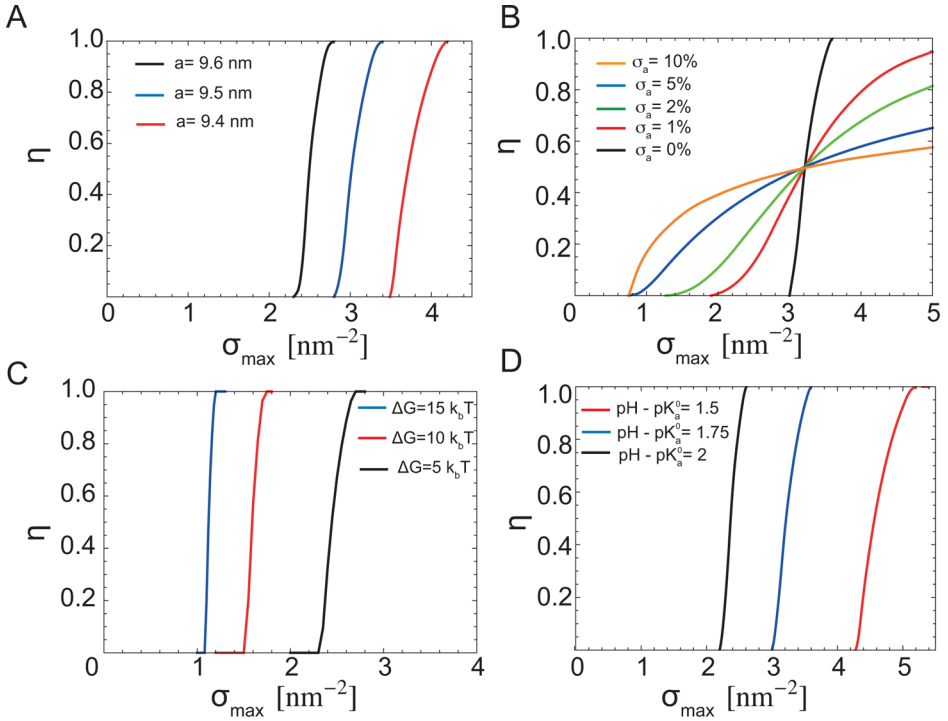

Figure 4. Encapsulation efficiency, η, as a function of the surface density of weakly acidic groups σ_{max} in the Debye−Hückel approximation, for (A) various radii of the nanoparticle a = 9.4, 9.5, and 9.6 nm, (B) various standard deviations σ_a of the size distribution, given a mean nanoparticle radius of (a) = 9.5 nm, (C) various values of the protein−protein binding free energy ΔG, and (D) different values of the acidity of the solution pH − pK_a^0. In these figures the nanoparticles are encapsulated by a T = 3 BMV capsid where we fixed b_{in} = 11.8 nm, λ_D = 1.2 nm, q = 90, $\varphi_{CP} = 1.8 \times 10^{-7}$, and $\varphi_{NP} = 2.0 \times 10^{-9}$. For part C a = 9.8 nm and for D a = 9.5 nm. For parts A, B, and D, ΔG = 0. For parts A, B, and C, pK_a^0 = 2.5 and pH = 4.5.

distribution of nanoparticles in our model,[3,5,22] we presume the following Gaussian probability density for nanoparticles with a radius between a and a + da

$$P(a) = \frac{1}{\sqrt{2\pi\sigma_a^2}} \exp\left(\frac{(a - (a))^2}{2\sigma_a^2}\right) \tag{12}$$

where σ_a is the standard deviation of the size distribution function and (a) the mean radius of the nanoparticles. Equation 1 then modifies to

$$\eta = \frac{\int_0^{b_{in}} P(a) \frac{(\phi_{CP}(1-\eta r)e^{-\Delta F(a)-\Delta G})^q}{1+(\phi_{CP}(1-\eta r)e^{-\Delta F(a)-\Delta G})^q} \, da}{\int_0^{b_{in}} P(a) \, da} \tag{13}$$

where $r = q\varphi_{NP}/\varphi_{CP}$ is the stoichiometric ratio and the CP−NP binding free energy ΔF now explicitly depends on the nanoparticle radius a. Obviously, in the limit of $\sigma_a \to 0$, eq 13 reduces to eq 1.

Figure 4B shows the encapsulation efficiency as a function of the surface density of chargeable groups σ_{max} for five different values of standard deviations (a), corresponding to 0%, 1%, 2%, 5%, and 10%, and a mean nanoparticle radius (a) = 9.5 nm. We presumed a T = 3-type BMV capsid and inserted the corresponding parameters,[17] b_{in} = 11.8 nm, q = 90, λ_D = 1.2 nm, $\varphi_{CP} = 1.8 \times 10^{-7}$, pK_a^0 = 2.5, and pH = 4.5. Since ΔG has little influence on σ_{max}, we set ΔG = 0 for simplicity.

We find within the Debye−Hückel approximation that a standard deviation as little as 1% already makes the increase of encaspulation efficiency as a function of σ_{max} more gradual. Furthermore, increasing the width of the size distribution also shifts the critical σ_{max} toward smaller values. This is because the larger particles from the tail of the distribution at lower values of σ_{max} contribute to the encapsulation efficiency (see Figure 4A). In addition we find that the saturation value of η decreases with increasing polydispersity because on one hand the smaller particles are too small to be encapsulated by BMV capsid proteins, while on the other hand larger particles require more proteins for encapsulation and as such they deplete the solution from available protein (a stoichiometric effect). This indicates that not only is the size of the nanoparticles an important experimental parameter but also their variation in size is, even if it is relatively narrow.

Protein−Protein Interactions. As we have discussed in the previous section, the protein−protein binding free energy, ΔG, is an experimentally accessible parameter.[12,27] To illustrate how it influences the encapsulation efficiency, we have calculated the efficiency for various values of ΔG, keeping all other system parameters constant, with a = 9.8 nm, b_{in} = 11.8 nm, q = 90, $\varphi_{CP} = 1.8 \times 10^{-7}$, $\varphi_{NP} = 2.0 \times 10^{-9}$, λ_D = 1.2 nm, pK_a^0 = 2.5, and pH = 4.5. In Figure 4C we see that, upon increasing the binding free energy between coat proteins, ΔG, from 0 to −15 k_BT, the critical σ_{max} above which assembly occurs decreases. This can be expected, as ΔG contributes to the total free energy upon encapsulation. The shape of the curves is again not strongly affected by the value of ΔG, which is also to be expected. In the next section, where we compare our model to the experimental data, we estimate the value of this model parameter based on recent literature.[12,27]

Validity of Debye−Hückel. The results presented above were obtained for the linearized Debye−Hückel approximation, whereas we have seen in the previous section that it can be quantitatively different from the semianalytical approach of the nonlinear Poisson−Boltzmann equation (described in the

DOI: 10.1021/jp5108125
J. Phys. Chem. B 2015, 119, 1869−1880

previous section). If we compare these two approaches for the same set of system parameters, the encapsulation efficiency as a function of σ_{max}, we find that the critical σ_{max} for the Debye–Hückel approximation is shifted, while the shape of the curve itself is very similar in both cases (see Figure 5). By shifting the radius of the nanoparticle with as little as 0.3 nm, the results from the semianalytical approach can be mapped on those of the Debye–Hückel approximation. This shows that, although not exact, the Debye–Hückel approximation describes the trend of the encapsulation efficiency quite well, at least for this specific system. In the following section we will present our main conclusions and compare our model with experimental data.[17]

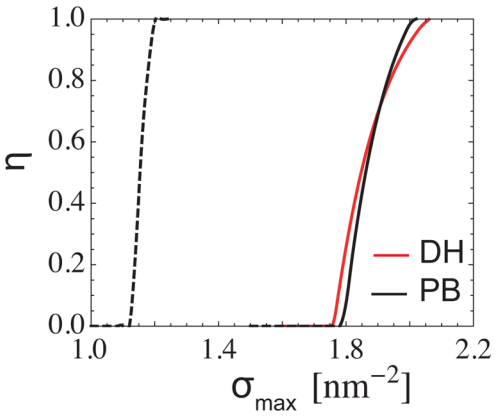

Figure 5. Encapsulation efficiency, η, as a function of the surface density of weakly acidic groups, σ_{max}, comparing the Debye–Hückel approximation (red curve) with the semianalytical treatment of the nonlinear Poisson–Boltzmann equation (black curves). For equal system parameters (a = 10.2 nm, b_{in} = 11.8 nm, b_{out} = 13.0 nm, q = 90, λ_D = 1.2 nm, φ_{CP} = 1.8 × 10^{-7}, pK_a^0 = 2.5, pH = 4.5, and ΔG = 0), it can be seen that the Debye–Hückel approximation (red curve) is shifted from the nonlinear Poisson–Boltzmann solution (dashed black curve), yet slightly decreasing the size of the nanoparticle with as little as a = 0.3 nm is sufficient to obtain a very similar encapsulation curve (solid black curve, a = 9.8 nm).

DISCUSSION AND CONCLUSIONS

We have compared our model with the experimental data of Daniel et al.,[17] who measured the encapsulation efficiency by BMV coat proteins of gold nanoparticles, end-grafted with carboxylated poly(ethylene glycol) (PEG). Particles of radius a = 4.7 nm, 6.25, and 8.1 nm were probed if we include a ligand coat thickness of 2 nm.[17] The experiments were performed at a pH of 4.5, at low ionic strength, corresponding to a Debye screening length of λ_D = 1.2 nm, ensuring that the encapsulation process is highly cooperative. The mole fraction of capsid proteins in aqueous solution of 1.8 × 10^{-7} was low enough for empty capsids not to form. At a fixed stoichiometric ratio of $r = \varphi_{CP}/q\varphi_{NP}$ = 1.33[17] protein depletion effects are not very significant even near full encapsulation efficiency. In the experiments, the mole fraction of nanoparticles was varied for different sizes of nanoparticle such that the stoichiometric ratio between protein and nanoparticles remained fixed. It appears that the 8.1 nm nanoparticles are encapulated by a T = 3 capsid, the 6.25 nm particles by a pseudo T = 2 capsid, and the 4.7 nm particles by a T = 1 capsid.[17]

To compare our model with the experiments, we also need to estimate the binding free energy between the coat proteins, ΔG for BMV and the bare pK_a^0 of the carboxylated PEGs. As the value for ΔG for BMV coat proteins in not known, we use the reported value $\Delta G = -17\ k_BT$ for the structurally related virus CCMV, measured under slightly different experimental conditions.[16] On the basis of previous theoretical work,[25] we expect ΔG to be slightly less negative for T = 1 and T = 2. However, we show in Figure 4 that a shift in ΔG only effects the critical surface charge density and not the shape of the curve. To this end, we will keep the value of ΔG fixed for the purpose of our calculations. There is no precise measurement for the bare pK_a^0 of the carboxylated PEGs as used in the experiments, at least to our knowledge. Similar molecules have a pK_a^0 around 2–3,[30] and therefore, we assume the bare pK_a^0 of these molecules to be 2.5. In fitting to the experimental data, we adjusted the inner and outer radius of the capsid protein shell too. This seems reasonable because the inner and outer surface of the capsid of BMV cannot be assumed to be perfectly spherical.[31] Moreover, the values we obtained for b_{in} and b_{out} are close to the values for BMV as reported in the literature.[31]

Figure 6a illustrates the experimentally obtained encapsulation efficiency (black dots with estimated error bars) for the encapsulation of a 8.1 nm nanoparticle by a T = 3 BMV capsid (inner capsid radius b_{in} = 11.3 nm, outer caspid radius b_{out} = 13.2 nm), and our theoretical findings based on the Debye–

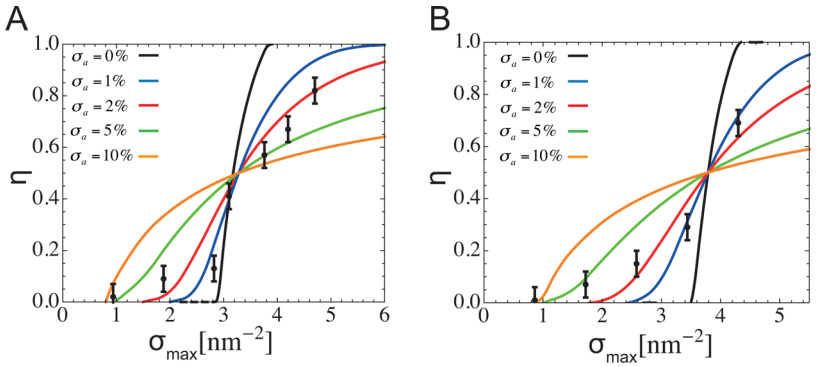

Figure 6. Encapsulation efficiency, η, as a function of the surface density of weakly acidic groups σ_{max}. Comparing the experimental data[17] (black dots) for (a) the nanoparticle with radius of a = 8.1 nm encapsulated by a T = 3 BMV capsid (b_{in} = 11.3 nm, b_{out} = 13.2 nm) and (b) the nanoparticle with radius of a = 6.25 nm encapsulated by a T = 2 BMV capsid (b_{in} = 8.8 nm, b_{out} = 10.0 nm). The stoichiometric ratio is r = 1.33, and the mole fraction of the protein dimer is in (a) 1.8 × 10^{-7} and in (b) 1.2 × 10^{-7}. In these fits we have fixed the binding free energy between the coat proteins ΔG = 17 k_BT per subunit, the pK_a^0 = 2.5, pH = 4.5, and the Debye screening length λ_D = 1.2 nm.

DOI: 10.1021/jp5108125
J. Phys. Chem. B 2015, 119, 1869–1880

Hückel model, for various standard deviations in nanoparticle size: σ_a = 0%,1%, 2%, 5%, and 10%. In Figure 6B, this procedure is repeated for the encapsulation of a 6.25 nm nanoparticle by a pseudo T = 2 BMV capsid (b_{in} = 8.8 nm, b_{out} = 10.0 nm). These results show our linearized Debye−Hückel model describes the experimental data for T = 2 and T = 3 very well for standard deviations in nanoparticle size of approximately 2−5%. For values of σ_a close to the experimental value 10%, our model shows even a more gradual increase of the encapsulation efficiency with increasing surface charge density, compared to the experimental data. In addition to this we find that, similar to the experiments, the encapsulation efficiency saturates at a value significantly smaller than 1. Our theoretical model was not able to accurately reproduce the T = 1 results within acceptable standard deviations of the nanoparticle size. This might indicate that the encapsulation of this size nanoparticle could be more accurately described by a Langmuir-type adsorption model rather than the Hill-type model that we have invoked above.

To summarize, we have compared Debye−Hückel theory with a semianalytical Poisson−Boltzmann theory to describe the electrostatics of the encapsulation of nanoparticles by virus coat proteins. We have seen that by slightly renormalizing system parameters, such as the nanoparticle radius, with as little as a few angstroms the two approaches could be mapped onto each other. A full numerical treatment of this problem, in combination with charge regulation and mass action, would come at high computational cost. Moreover, the extreme sensitivity of both the linear and nonlinear Poisson−Boltzmann theory toward nanoparticle size, capsid size, binding free energy, and surface charge density, raises the question whether a full numerical treatment of the coarse-grained model on an atomistic description is actually sensible. Arguably, small perturbations in nanoparticle size or even thermal effects could dramatically impact predictions. In addition to this, previous work[22] has shown that the encapsulation is also highly affected by the natural variation in the density of chargeable surface groups on the nanoparticle, making it even more challenging to theoretically predict the outcome of encapsulation experiments. Charge regulation of the weakly acidic groups suggests that the use of strong acids would allow for more accurate control over the effective surface charges on the surface of nanoparticles and hence the encapsulation.

Theoretical descriptions of the role of electrostatics in the encapsulation of functionalized nanoparticles by viral coat proteins, based on Poisson−Boltzmann (or Debye−Hückel) theory,[3,5,21,22] have rationalized many experimental findings presented in the work of Dragnea and collaborators.[17] While the previous theoretical work has shed light on the fact that increasing surface charge density beyond a certain critical value results in a gradual increase in the encapsulation efficiency of nanoparticles, some aspects of experimental data remain unexplained.

In this work we have included the mechanism known as charge regulation in our electrostatic description of the self-assembly of capsid coat proteins around nanoparticles and accounted for the natural polydispersity in nanoparticle size that were previously ignored. The former controls the number of charged groups on the surface of the nanoparticle and optimizes the electrostatic free energy. Its impact depends strongly on the surface density of chargeable groups, the pH of the solution, and the number of charges present on the RNA-binding domain of the proteins. An important consequence of charge regulation is that the number of charged groups is larger for an encapsulated nanoparticle compared to that of a free nanoparticle. It follows that the effective pK_a of the surface groups of the nanoparticles depends on their electrostatic environment.

A second main result of our work is that the encapsulation efficiency sensitively depends upon the radius of the nanoparticles relative to that of the inner caspid radius. As a consequence, the natural variation in nanoparticle size, i.e., the size polydispersity, significantly shifts the critical surface density of chargeable groups above which nanoparticles are encapsulated. A standard deviation in nanoparticle size as little as 1% makes the dependence of the encapsulation efficiency on the surface density of chargeable groups more gradual, and as such, the encapsulation appears much less cooperative than it is. We find this effect for both the Debye−Hückel and the Poisson−Boltzmann theory. For the conditions tested the results obtained for both theories are numerically different for the same parameter values, but we find they can be made to superimpose by a very small renormalization of the nanoparticle size.

Our results also strongly suggest that not only the size of the nanoparticle but also the size of the capsid protein itself, and hence any natural variation in it, even when small, significantly influences the encapsulation efficiency. This has far-reaching concequences for the practical application of designing protein cages for encapsulation, where control of capsid size is crucial. Hence, a greater understanding of the mechanisms underlying the virus assembly should have a significant impact on areas of material science and medical nanotechnology.

APPENDIX A

Electrostatic Interactions

In this appendix we outline the calculations of the electrostatic potential we invoked in the main text. The electrostatic potential of a negatively charged sphere, surrounded by positively charged layer, in the presence of a 1:1 electrolyte, can be calculated from the Poisson−Boltzmann equation

$$\nabla^2\psi(\bar{r}) = \lambda_D^{-2}\sinh(\psi(\bar{r})) - 4\pi\lambda_B\rho \tag{14}$$

where $\psi(\bar{r})$ is the dimensionless electrostatic potential at position $\bar{r}$, ρ the volume charge density associated with the charges on the RNA-binding domain, and λ_D the Debye length $\lambda_D = 1/(8\pi\rho_0\lambda_B)^{1/2}$, which is a measure of the electrical screening length and is inversely proportional to the square root of the salt density ρ_0. Here $\lambda_B = \beta e^2/4\pi\varepsilon$ is the Bjerrum length, the distance over which the electrostatic interaction between two elementary charges e is equal in magnitude to the thermal energy k_BT.

As the electrostatic potential for this specific geometry cannot be solved analytically we make use of an approximation, valid within the limit $\psi \ll 1$. In this so-called Debye−Hückel approximation we linearize $\sinh \beta e\psi$. Besides this linear analysis we also invoke a semianalytical approach of the nonlinear Poisson−Boltzmann equation, based on descriptions by Prinsen et al.[25] for multishell capsids and by Tuinier[29] for charged spherical particles for fixed surface charge density. In the remainder of this appendix we will describe these two approaches.

Debye−Hückel Approximation

For an encapsulated nanoparticle with a nanoparticle radius a, inner capsid radius b_{in}, outer capsid radius b_{out}, and Q_v charges

DOI: 10.1021/jp5108125
J. Phys. Chem. B 2015, 119, 1869−1880

in the RNA-binding domain, the electrostatic potential, within the Debye Hückel approximation, is obtained by solving the linearized form of eq 14, resulting in

$$\psi_1(a < x < b_{in}) = (C_1/x)\exp(-x/\lambda_D) + (C_2/x)\exp(x/\lambda_D) + \frac{3Q_v\lambda_D}{b_{in}^3 - a^3}$$
$$\psi_2(b_{in} < x < b_{out}) = C_2\frac{b_{in}}{x}\frac{b_{out} - x}{b_{out} - b_{in}} + C_2\frac{b_{out}}{x}\frac{b_{in} - x}{b_{out} - b_{in}}$$
$$\psi_3(x > b_{out}) = (C_3/x)\exp(-x/\lambda_D) \quad (15)$$

where the constants C_1, C_2, and C_3 can be obtained by applying the boundary conditions

$$\frac{1}{\lambda_B}\psi_1'(b_{in}) = -4\pi f\sigma_{max}$$
$$\frac{1}{\lambda_B^p}\psi_1'(b_{in}) - \frac{1}{\lambda_B}\psi_2'(b_{in}) = 0$$
$$\frac{1}{\lambda_B}\psi_2'(b_{out}) - \frac{1}{\lambda_B^p}\psi_3'(b_{out}) = 0 \quad (16)$$

where σ_{max} is the surface density of weak acidic groups, f the fraction of deprotonated groups, λ_B^p the Bjerrum length within the capsid domain, and λ_B the Bjerrum length within the RNA-binding domain and outside the capsid domain. We assume the λ_B^p is a factor of 16 larger in the protein shell compared to that in water (λ_B).[25]

The reference state of the encapsulated nanoparticle consists of a free nanoparticle and q free protein subunits, where q is the number of coat proteins necessary to encapsulate one nanoparticle. The electrostatic potential for a free nanoparticle, within the Debye–Hückel approach, is given by

$$\psi(x) = (C_1/x)e^{-(x-a)/\lambda_D} \quad (17)$$

The constant C_1 is determined by applying the following boundary conditions

$$\frac{d\psi(a)}{dx} = -4\pi\lambda_B f\sigma_{max} \quad (18)$$
$$\psi(\infty) = 0 \quad (19)$$

in which $f\sigma_{max}$ is the surface charge density and a the radius of the nanoparticle. Applying these boundary conditions results in

$$C_1: = \frac{4\pi a^2\lambda_B\lambda_D}{(\lambda_D + a)}f\sigma_{max} \quad (20)$$

This approximate solution is valid for low surface charge density.

The second component of the reference state is the free capsid proteins. These capsid proteins are modelled as spherical particles containing the RNA-binding domain, having Q_a charges and a dimensionless radius r_a, which is determined by free energy minimalization. The electrostatic potential of this system is determined by solving the linearized version of eq 14 for a homogeneously charged sphere with a total charge Q_a. The solution inside the spherical particles $x < r_a$ is given by

$$\psi_1(x) = (C_1/x)\sinh(x/\lambda_D) + \frac{3Q_a\lambda_B\lambda_D^2}{r_a^3} \quad (21)$$

and outside the particle, $x > r_a$, by

$$\psi_2(x) = (C_2/x)e^{-(x-r_a)/\lambda_D} \quad (22)$$

The constants C_1 and C_2 can be determined by applying the following boundary conditions

$$\psi_1(r_a) = \psi_2(r_a) \quad (23)$$
$$\frac{d\psi_1(r_a)}{dx} = \frac{d\psi_2(r_a)}{dx} \quad (24)$$
$$\psi_2(\infty) = 0 \quad (25)$$

resulting in

$$C_1: = \frac{3\lambda_D^2(r_a + \lambda_D)}{r_a^3}Q_a \quad (26)$$
$$C_2: = \frac{3\lambda_D^2(r_a - 0.5(r_a + \lambda_D)(1 + e^{-2r_a/\lambda_D})}{r_a^3}Q_a \quad (27)$$

Semianalytical Analysis

Apart from the Debye–Hückel approximation described in the previous section, we make use of a limiting case of the multishell structure described in Prinsen et al.[25] to model the encapsulated nanoparticle. This approach hinges on the fact that the total number of fixed charges in the RNA-binding region is much larger than that of the mobile ions due to counter ion release, allowing us to treat the influence of the latter on the local electrostatic potential perturbatively. The interior of the protein shell itself is assumed to contain no free charges, so in this region the problem reduces to a Poisson problem. Outside the capsid, the electrostatic potential is sufficiently small to allow for a Debye–Hückel approximation.

The potential in the region $a < x < b_{in}$ is given by

$$\psi_1(x) = \psi_0 + C_1\frac{a}{x}\frac{\sinh[\alpha(b_{in} - x)/\lambda_D]}{\sinh[\alpha(b_{in} - a)/\lambda_D]} + C_2\frac{b_{in}}{x}\frac{\sinh[\alpha(x - a)/\lambda_D]}{\sinh[\alpha(b_{in} - a)/\lambda_D]} \quad (28)$$

where

$$\psi_0 = \operatorname{arcsinh}(\rho_1/c_0) \quad (29)$$

and

$$\alpha = \operatorname{arcsinh}(\cosh\psi_0) \quad (30)$$

where ρ_1 is the charge density of the RNA binding domain and c_0 the concentration of monovalent salt. Inside the coat protein, there are no free ions present, which results in

$$\psi_2(x) = (C_2 + \psi_0)\frac{b_{in}}{x}\frac{b_{out} - x}{b_{out} - b_{in}} + C_3\frac{b_{out}}{x}\frac{x - b_{in}}{b_{out} - b_{in}} \quad (31)$$

Outside this region ($x > b_{out}$), the Debye–Hückel approach is valid

$$\psi_3(x) = (\psi_0 + C_3)\frac{b_{out}}{x}e^{-(x-b_{out})/\lambda_D} \quad (32)$$

The constants C_1, C_2, and C_3 can be determined using the same boundary conditions as in the Debye–Hückel approach.

To model the free nanoparticle, we follow an approach proposed by Tuinier.[29] This solution uses the analytical solution of the Poisson-Boltzmann equation for a flat geometry

DOI: 10.1021/jp5108125
J. Phys. Chem. B 2015, 119, 1869–1880

as ansatz and multiplies it with an ad hoc curvature term $a/(a + x)$. The solution for a spherical particle with radius a is given by

$$\psi(x) = \frac{2a}{x}\ln\left(\frac{1 + t_0 e^{-(x-a)/\lambda_D}}{1 - t_0 e^{-(x-a)/\lambda_D}}\right) \quad (33)$$

where $t_0 = \tanh[\psi(a)/4]$ and $\Psi(a)$, the electrostatic potential at the surface of the spherical particle. Because the surface potential is unknown, a relation should be derived between the surface potential and the surface charge density. An exact relation between the dimensionless surface potential $\psi(a)$ and the dimensionless surface charge density $f\sigma_{max}$ for a flat surface is given by

$$\psi(a) = 2\ln(2\pi\lambda_B^2\sigma + \sqrt{(2\pi\lambda_B\sigma)^2 + 1}) \quad (34)$$

Inserting this relation into eq 33, and comparing it with the numerical solution of the Poisson−Boltzmann equation, results in an excellent agreement for particles for which $a/\lambda_D > 2$ and independent of σ and λ_D as shown by Tuinier.[29]

Apart from the free nanoparticle, our reference state consists of q RNA-binding domains free in solution. As their charge density is relatively small we will use the Debye−Hückel approximation described in the previous section.

Free Energy Calculation

The electrostatic free energy we calculated uses the thermodynamic integration method as described by Loeb and Overbeek[32]

$$F_C = \int \rho\psi(\vec{r}, \rho)dV + \int \sigma_{max} f\psi(\vec{r}, \sigma_{max}f)\, dS \quad (35)$$

where we calculate the fraction of charged surface groups f by minimizing this electrostatic free energy. This is equivalent to summing the electrostatic contribution of the charged regions and adding the translational entropy of the salt ions separately as was done in, e.g., Prinsen et al.[25] for electrostatic potentials derived from the Poisson−Boltzmann equation. Predictions differ, however, if the potentiaal inserted are not exact solutions of the Poisson−Boltzmann equation.

As mentioned above, the free energy of the RNA-binding domain of the free proteins subunits strongly depends on their equilibrium radius. This is determined by the competition between repulsive electrostatic interactions and the entropic interactions of the ARM, which are modelled as Gaussian springs. To determine the equilibrium radius the ARMs, they are modeled as freely rotating chains consisting of three segments per amino acid, each of length a_a.[25] The entropic free energy contribution of the ideal chain is given by

$$F_{ent} = \frac{3r_e^2}{2r_a^2} + \frac{3r_a^2}{2r_e^2} \quad (36)$$

where r_e^2 is the average square end-to-end distance of the isolated chain in equilibrium, which is given by $r_e^2 \approx 2.56na^2$ for a freely rotating chain consisting of n segments of length a and a bond angle between the segments of 116°.[25] We use this competition between the electrostatic free energy of the RNA-binding domain and the entropic free energy to determine the equilibrium radius following

$$\frac{\partial(F_C + F_{ent})}{\partial r}\Big|_{r=r_a} = 0 \quad (37)$$

For BMV caspid protein, a single RNA-binding dimer has Q_A = 18 charges/dimer and a domain length of 2 times 20 amino acids.[31] Using eq 37, the free energy is minimized for a radius $r_A \approx 6.7$ nm, given a Debye length of $\lambda_D = 1.2$ nm. The electrostatic part of the free energy of such a dimer corresponds to approximately $3k_BT$.

AUTHOR INFORMATION

Corresponding Author

*E-mail: p.p.a.m.v.d.schoot@tue.nl.

Notes

The authors declare no competing financial interest.

ACKNOWLEDGMENTS

The authors gratefully acknowledge funding from the International Human Frontier Science Program Organization (B.D. and P.v.d.S.) and the National Science Foundation through Grant DMR-1310687 (R.Z.).

REFERENCES

(1) McPherson, A. Micelle Formation and Crystallization as Paradigms for Virus Assembly. *BioEssays* **2005**, *27*, 447−458.

(2) van der Schoot, P.; Bruinsma, R. Electrostatics and the Assembly of an RNA virus. *Phys. Rev. E* **2005**, *71*, 619−628.

(3) Hagan, M. A Theory for Viral Capsid Assembly Around Electrostatic Cores. *J. Chem. Phys.* **2009**, *130*, 114902.

(4) Belyi, V. A.; Muthukumar, M. Electrostatic Origin of the Genome Packing in Viruses. *Proc. Natl. Acad. Sci. U.S.A.* **2006**, *103*, 17174−17178.

(5) Šiber, A.; Zandi, R.; Podgornik, R. Thermodynamics of Nanospheres Encapsulated in Virus Capsids. *Phys. Rev. E* **2010**, *81*, 051919.

(6) Rao, Z.; Belyaev, A. S.; Fry, E.; Roy, P.; Jones, I. M.; Stuart, D. I. Crystal Structure of SIV Matrix Antigen and Implications for Virus Assembly. *Nature* **1995**, *378*, 743−747.

(7) Stockley, P. G.; Rolfsson, O.; Thompson, G. S.; Basnak, G.; Francese, S.; Stonehouse, N. J.; Homans, S. W.; Ashcroft, A. E. A Simple, RNA-Mediated Allosteric Switch Controls the Pathway to Formation of a T = 3 Viral Capsid. *J. Mol. Biol.* **2007**, *369*, 541−552.

(8) Twarock, R. Mathematical Virology: a Novel Approach to the Structure and Assembly of Viruses. *Philos. Trans R. Soc., A.* **2006**, *364*, 3357−3373.

(9) Bancroft, J. In *The Self-Assembly Of Spherical Plant Viruses*; Kenneth, M., Smith, M. A. L., Bang, F. B., Eds.; Advances in Virus Research; Academic Press: New York, 1970; Vol. *16*; pp 99 − 134.

(10) Cadena-Nava, R. D.; Hu, Y.; Garmann, R. F.; Ng, B.; Zelikin, A. N.; Knobler, C. M.; Gelbart, W. M. Exploiting Fluorescent Polymers To Probe the Self-Assembly of Virus-like Particles. *J. Phys. Chem. B* **2011**, *115*, 2386−2391.

(11) Aniagyei, S. E.; DuFort, C.; Kao, C. C.; Dragnea, B. Self-Assembly Approaches to Nanomaterial Encapsulation in Viral Protein Cages. *J. Mater. Chem.* **2008**, *18*, 3763−3774.

(12) Ceres, P.; Zlotnick, A. Weak Protein Protein Interactions Are Sufficient To Drive Assembly of Hepatitis B Virus Capsids. *Biochemistry* **2002**, *41*, 11525−11531.

(13) Kwak, M.; Minten, I. J.; Anaya, D.-M.; Musser, A. J.; Brasch, M.; Nolte, R. J. M.; Müllen, K.; Cornelissen, J. J. L. M.; Herrmann, A. Virus-like Particles Templated by DNA Micelles: A General Method for Loading Virus Nanocarriers. *J. Am. Chem. Soc.* **2010**, *132*, 7834−7835.

(14) Ma, Y.; Nolte, R. J.; Cornelissen, J. J. Virus-Based Nanocarriers for Drug Delivery. *Adv. Drug Delivery Rev.* **2012**, *64*, 811−825.

(15) Sun, J.; DuFort, C.; Daniel, M.-C.; Murali, A.; Chen, C.; Gopinath, K.; Stein, B.; De, M.; Rotello, V. M.; Holzenburg, A.; Kao, C. C.; Dragnea, B. Core-Controlled Polymorphism in Virus-like Particles. *Proc. Natl. Acad. Sci. U.S.A.* **2007**, *104*, 1354−1359.

(16) Tsvetkova, I.; Chen, C.; Rana, S.; Kao, C. C.; Rotello, V. M.; Dragnea, B. Pathway Switching in Templated Virus-Like Particle Assembly. *Soft Matter* **2012**, *8*, 4571−4577.

DOI: 10.1021/jp5108125
J. Phys. Chem. B 2015, 119, 1869−1880

(17) Daniel, M.; Tsvetkova, I.; Quinkert, Z.; Murali, A.; Rotello, V.; Kao, C.; Dragnea, B. Role of Surface Charge Density in Nanoparticle-Templated Assembly of Bromovirus Protein Cages. *ACS Nano* **2010**, *4*, 3853.
(18) Dixit, S. K.; Goicochea, N. L.; Daniel, M.-C.; Murali, A.; Bronstein, L.; De, M.; Stein, B.; Rotello, V. M.; Kao, C. C.; Dragnea, B. Quantum Dot Encapsulation in Viral Capsids. *Nano Lett.* **2006**, *6*, 1993−1999.
(19) Chen, C.; Daniel, M.-C.; Quinkert, Z. T.; De, M.; Stein, B.; Bowman, V. D.; Chipman, P. R.; Rotello, V. M.; Kao, C. C.; Dragnea, B. Nanoparticle-Templated Assembly of Viral Protein Cages. *Nano Lett.* **2006**, *6*, 611−615.
(20) Wang, D.; Nap, R. J.; Lagzi, I.; Kowalczyk, B.; Han, S.; Grzybowski, B. A.; Szleifer, I. How and Why Nanoparticle's Curvature Regulates the Apparent pKa of the Coating Ligands. *J. Am. Chem. Soc.* **2011**, *133*, 2192−2197.
(21) Šiber, A.; Podgornik, R. Role of Electrostatic Interactions in the Assembly of Empty Spherical Viral Capsids. *Phys. Rev. E* **2007**, *76*, 061906.
(22) Lin, H.-K.; van der Schoot, P.; Zandi, R. Impact of Charge Variation on the Encapsulation of Nanoparticles by Virus Coat Proteins. *Phys. Biol.* **2012**, *9*, 066004.
(23) Zandi, R.; van der Schoot, P. Size Regulation of ss-RNA Viruses. *Biophys. J.* **2009**, *96*, 9−20.
(24) Lund, M.; Jönsson, B. On the Charge Regulation of Proteins. *Biochemistry* **2005**, *44*, 5722−5727.
(25) Prinsen, P.; van der Schoot, P.; Gelbart, W.; Knobler, C. Multishell Structures of Virus Coat Proteins. *J. Phys. Chem. B* **2010**, *114*, 5522−5533.
(26) He, L.; Porterfield, Z.; van der Schoot, P.; Zlotnick, A.; Dragnea, B. Hepatitis Virus Capsid Polymorph Stability Depends on Encapsulated Cargo Size. *ACS Nano* **2013**, *7*, 8447−8454.
(27) Kegel, W. K.; van der Schoot, P. Competing Hydrophobic and Screened-Coulomb Interactions in Hepatitis B Virus Capsid Assembly. *Biophys. J.* **2004**, *86*, 3905−3913.
(28) Lund, M.; Jönsson, B. Charge Regulation in Biomolecular Solution. *Q. Rev. Biophys.* **2013**, *46*, 265−281.
(29) Tuinier, R. Approximate Solutions to the Poisson Boltzmann Equation in Spherical and Cylindrical Geometry. *J. Colloid Interface Sci.* **2003**, *258*, 45−49.
(30) Ripin, D. H.; Evans, D. A. pKa's of Inorganic and Oxo-Acids. http://www.chem.wisc.edu/areas/reich/pkatable/index.html (accessed Jan 5, 2014).
(31) Lucas, R. W.; Larson, S. B.; McPherson, A. The Crystallographic Structure of Brome Mosaic Virus. *J. Mol. Biol.* **2002**, *317*, 95−108.
(32) Loeb, A. L.; Wiersema, P.; Overbeek, J. T. G. *The Electrical Double Layer Around a Spherical Colloid Particle: Computation of the Potential Charge Density, and Free Energy of the Electrical Double Layer Around a Spherical Colloid Particle*; MIT Press: Cambridge, MA, 1961.

DOI: 10.1021/jp5108125
J. Phys. Chem. B 2015, 119, 1869−1880